



4D printing parameters optimisation for bi-stable soft robotic gripper design

Ali Zolfagharian¹ · Mohammad Lakhi^{1,2} · Sadegh Ranjbar³ · Morteza Sayah Irani⁴ · Marwan Nafea⁵ · Mahdi Bodaghi⁶

Received: 28 December 2022 / Accepted: 17 March 2023 / Published online: 29 March 2023
© The Author(s) 2023

Abstract

Four-dimensional (4D) printing is an emerging additive manufacturing (AM) technology that adds a time-dependent reconfiguration dimension to three-dimensional (3D) printed products. It enables the creation of on-demand, dynamically controllable shapes, or properties in response to external stimuli such as temperature, magnetic field, and light. Thermally responsive structures are among the most popular types of currently available 4D-printed structures due to their convenience. However, applications like soft robots are hindered by the temperature-sensitive structures' stagnating actuation. This research was driven by a requirement for a rapid and effective design and optimisation strategy for 4D-printed bi-stable thermally responsive structures for use in soft robotics. In this study, the response surface method (RSM) optimization with the aid of numerical solutions was used to investigate effective parameters in the design of a bi-stable, 4D-printed soft robotic gripper. This approach is proposed to accelerate the actuation of thermally responsive shape-morphing structures that can be controlled by the in situ strains and post-manufacturing heat stimuli as variable parameters. By using RSM solution the individual effects as well as the coupling effects of variable parameters on the output responses, including the maximum strain energy and the average distance between the clamps of the structure, are evaluated. The obtained results can be employed to develop the designation and improve the acceleration of soft robotic grippers such as fast buckling and bending, which is desirable for soft robotic applications.

Technical Editor: Jovana Jovanova.

✉ Ali Zolfagharian
a.zolfagharian@deakin.edu.au

¹ School of Engineering, Deakin University, Geelong, VIC 3216, Australia

² Department of Mechanical Engineering, Birjand University of Technology, Birjand, Iran

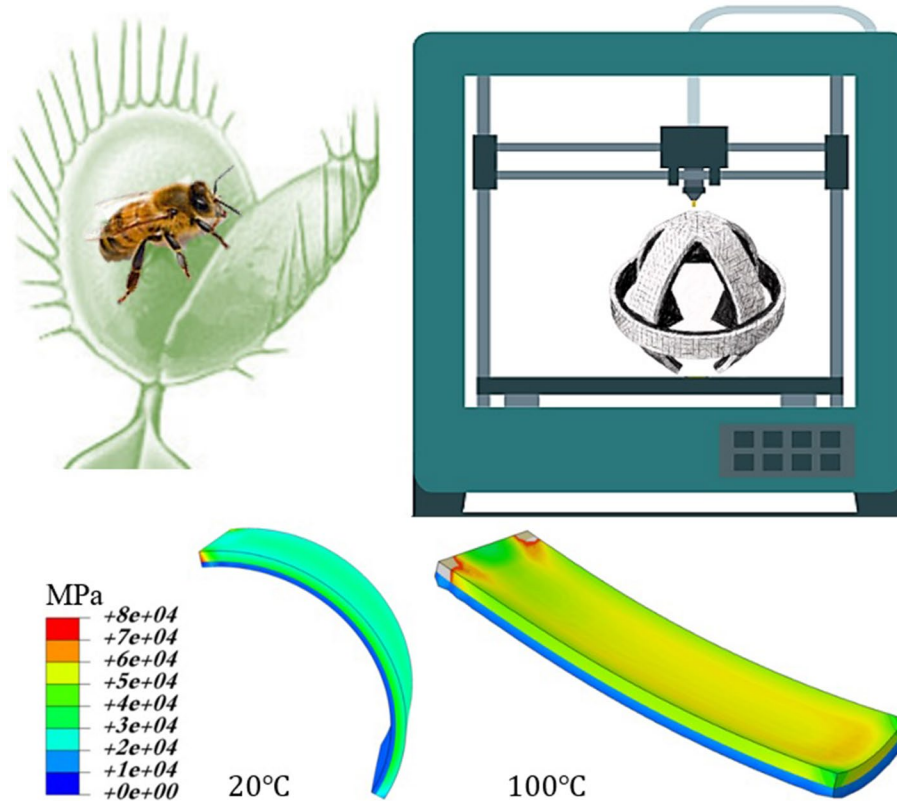
³ Department of Mechanical Engineering, Faculty of Engineering, Urmia University, Urmia, Iran

⁴ Department of Mechanical Engineering, University of Birjand, Birjand, Iran

⁵ Department of Electrical and Electronic Engineering, Faculty of Science and Engineering, University of Nottingham Malaysia, 43500 Semenyih, Selangor, Malaysia

⁶ Department of Engineering, School of Science and Technology, Nottingham Trent University, Nottingham NG11 8NS, UK

Graphical abstract



Keywords Response surface method (RSM) · 4D printing · Pre-strain · Silicone · Finite element method (FEM)

1 Introduction

The use of smart materials in additive manufacturing (AM) and four-dimensional (4D) printing has recently become much more feasible due to advancements in synthetic smart materials, new printers, and mathematical modelling [1, 2]. The ability to reassemble simple components into a complex structure that cannot be built with existing manufacturing technologies is a notable case of the design flexibility enabled by 4D printing. Robots [3], automobiles [4], healthcare [5], and aerospace [6] are just some of the emerging markets for three-dimensional (3D) printing technologies, and there has also been a notable shift towards using 4D printing technology to create soft robotics for use in a multitude of environments. The field of soft robotics is a relatively new area of study, with much of the current research being inspired by the systems in nature that have been modified over generations to achieve a certain purpose. Since rigid robots are often constructed from inflexible materials, they are unable to bend and conform elastically, just as a mouse or octopus can squeeze through a small hole without causing detrimental internal

pressures and stress concentrations, to overcome physical impediments [7].

However, soft robotics introduces an interesting new paradigm in engineering that drives us to re-evaluate how we develop materials and mechanisms to make them more practical, versatile, and adaptive in various interactions [8]. Closed-loop 4D-printed soft robots [5, 9] were introduced with potential applications in food sorting [9] and autonomous surgeries [10], which conventional robots are challenged to handle [11]. Finite element method (FEM) and 4D printing techniques are necessary for designing a closed-loop soft robot to attain a targeted design suitable for a practical application due to the varying physical responses of the integrated materials [9]. Tawk et al. [12] used FEM to improve the gripper's soft fingers. It was shown that the FE simulations were successful in improving the gripper's performance by precisely predicting the fingers' behaviour and performance in terms of deformation and tip force. A novel design method was proposed by Chau et al. [13] to address the issue of structural optimisation for the soft rotary joint. The adaptive neuro-fuzzy inference system model, the FEM, and the water cycle moth-flame optimisation algorithm all

contributed to the development of the suggested optimisation method. Taguchi approach was used to optimise the neuro-fuzzy inference system adaptively, which improves the precision of the models produced. However, all these methods were performed on 3D-printed soft grippers and robots without consideration of their 4D or stimuli-responsive properties in the optimization stage.

Recently, there has been a practical yet efficient 4D printing technique for developing soft grippers via pre-strain induced during the fabrication mechanism. A 4D printing platform was developed by Zou et al. [14], which can apply strain during the printing process to fabricate the pre-strained structures with the aid of in situ the printing base. When printing a bilayer construction, one layer is pre-strained, while the other is not. Experiments and FEM demonstrated that the aspect ratio has little influence on the deformation of the bilayer structure; however, the pre-strain plays a crucial role in the deformation and significantly speeds up the actuation of the bilayer structure. Using this method, a 4D-printed pre-strained bilayer energy-free gripper was fabricated. In another work, a 4D printing method for fabricating multiscale shape-morphing structures was presented by Deng et al. [15], which can be precisely controlled by the applied strains. To create these prototypes, a two-nozzle 3D printer was used to print phase change wax microparticles (MPs) into the elastomer matrix. Because of the solid–liquid phase shift, the wax MPs are able to keep the residual strain after the pre-strained elastomer composite has been relaxed. The anisotropic stress field in the elastomer composite is achieved by the 3D-programmable spatial distribution of the wax MPs. These stresses result in out-of-plane deformations such as curling, folding, and buckling. Due to the reversible phase transition of the wax MPs, these deformations are multiscale and programmable. It was also reported that the characteristics of deformations, such as curvatures and folding angles, are linearly dependent on the applied strains, suggesting controllable features. Furthermore, the bi-stable mechanism was incorporated into the pre-strain 4D printing principle by Liu et al. [16] in a soft and bi-stable gripper. It was shown that the gripper deforms upon impact with other objects, absorbing their kinetic energy to provide instability and allowing for both rapid gripping and a degree of cushioning. Since this method does not need any additional energy input, it substantially simplifies the usual driving devices allowing for the miniaturised and lightweight gripping actuation to be achieved. By applying the right amount of pre-deformation to the gripper's bi-stable structure, the energy barrier for initiating the beginning of instability may be dynamically adjusted to provide the best possible grasp and buffering effect, as per the target's kinetic properties. As soon as it has completed its current gripping task, the bi-stable gripper may reset to its starting position and release the object using a cable-driven

mechanism. Their experiment shows the suggested soft gripper could grab, transport, and release moving items, giving it considerable potential to carry out tricky activities on space missions.

All recent studies have demonstrated the feasibility and utility of 4D printing in the development of soft grippers with pre-strain and bi-stable mechanisms. However, there was little effort focused on the optimization of the parameters to accelerate the actuation of thermally responsive structures. In this research, we use the response surface method (RSM) optimization with the aid of numerical solutions to investigate effective parameters in the design of a bi-stable, 4D-printed soft robotic gripper. The bi-stability is induced based on the pre-strain 4D printing mechanism in the soft gripper. This approach is proposed to accelerate the actuation of thermally responsive shape-morphing structures that can be controlled by the applied strains during the manufacturing and post-manufacturing heat stimuli as variable parameters.

2 Methodology

2.1 Design and formulation

In this research, a pre-strained bilayer thermal actuator is evaluated according to the recent development in [14, 16], as shown in Fig. 1, due to its fast actuation mechanism. The 4D printing procedure is the same as earlier work of authors [14, 17]. Based on this characteristic, these actuators can be effectively used in soft robotic grippers, as the variation in curvature of the structure can be considered an appropriate parameter for the effective deformation calculation of pre-strained bilayer structures. Liu et al. [16] also presented a designation for the bi-stable soft robotic grippers used for the dynamic capture of objects in space. As shown in Fig. 1b, they used a particular design consisting of a normal soft gripper and a ring, which causes the structure to be bi-stable. Based on the research background, one of the criteria to evaluate the stability of bi-stable soft robotic grippers is the amount of strain energy created in the gripper [18]. It should be noted that in most studies, the silicone elastomer processed by 3D printing is used to fabricate gripper samples [14, 16].

Based on what was explained about soft grippers, FEM is used in the current study to investigate the pre-strain effect of the bilayer structure with various thickness ratios on the performance of the 4D-printed bi-stable soft robotic gripper. A design process of and analysis procedure in this study could be seen in Fig. 2 flowchart. As can be seen from the flowchart in Fig. 2, the study begins by investigating the effective parameters according to the literature review. The design of experiments (DoE) is then conducted, followed

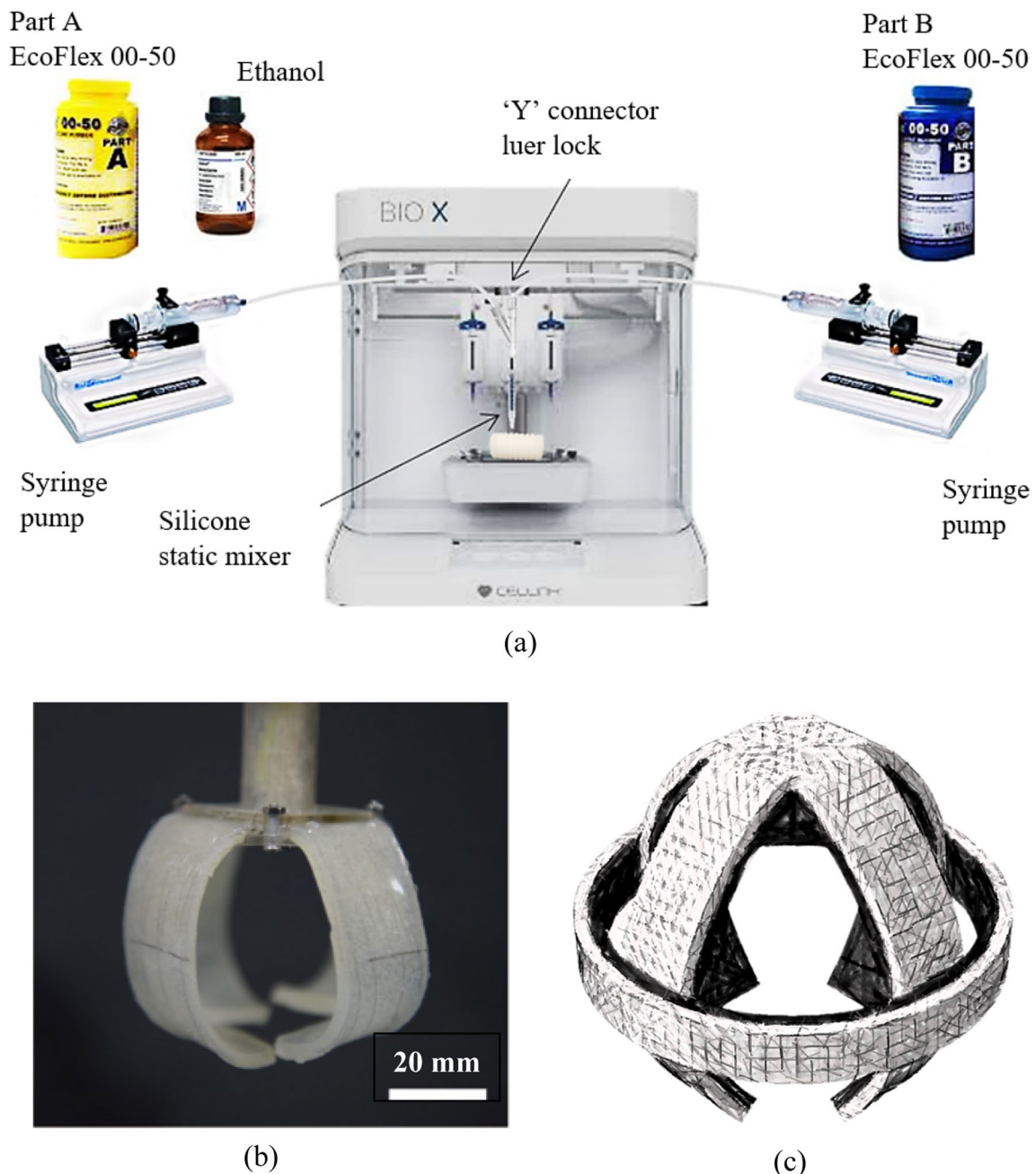


Fig. 1 **a** The 3D printing procedure of the thermally responsive actuator described in the earlier work of the authors [17], adapted with permission from IOP; the bi-stable soft robotic gripper **(a)** without

the constrained ring [14], adapted under a Creative Commons Attribution (CC BY) license from Frontiers; and **b** with the constrained ring in this work

by the geometric design of a soft gripper by the CATIA V5 software. Next, the simulation of a soft gripper by ABAQUS 2017 software is carried out, followed by extracting simulation results and determining output values. Finally, RSM modelling and optimization results are done in the MATLAB-R2021a software.

For this purpose, the bi-stable gripper sample was designed similarly to that of the gripper in [16], as shown

in Fig. 2. The structure of the bi-stable soft robotic gripper was considered a two-layer structure with specified pre-strain values and thickness ratios, consisting of one layer of silicone–ethanol composite and one layer of silicone elastomer. The thermomechanical properties of silicone–ethanol and silicone elastomer are reported in Table 1. It should be noted that silicone–ethanol composite is a relatively soft and flexible material that could be isotopically deformed

Fig. 2 The design process of and analysis procedure in this study

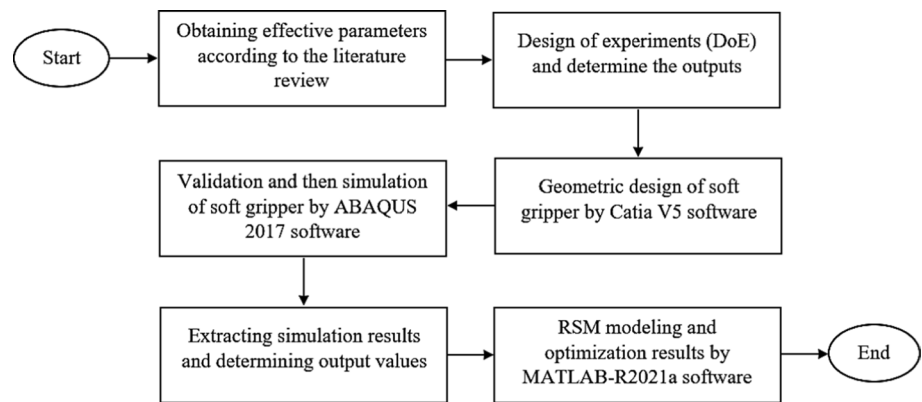


Table 1 Properties of materials used in the 4D-printed bi-stable soft robotic gripper

Material	Properties					
	Density (Kg/m ³)	Young's modulus (MPa)	Poisson's ratio (–)	Thermal expansion coefficient (K ⁻¹)	Thermal conductivity (W/m K)	Specific heat (JM ⁻¹ θ ⁻¹)
Silicone–ethanol	1100	0.052	0.45	0.0025	0.4	1.9
Silicone elastomer	970	2	0.45	≈ 0	0.15	1.46

under thermal stimulation, but silicone elastomer demonstrates almost no expansion under thermal stimulation and it has a high Young's modulus compared to silicone–ethanol composite [19].

By using Model-Based Calibration (MBC) Model Fitting Toolbox in MATLAB R2021a software, the design of experiments was done based on RSM methodology, which includes three-level input parameters and two output parameters. It also should be mentioned that two modes were considered for the soft robotic gripper designation. In the first mode, the soft gripper consists of a silicone–ethanol composite material with a high coefficient of thermal expansion in the outer layer and a silicone elastomer with a low coefficient of thermal expansion in the inner layer. In the second mode, the order of locating the layers is reversed. Concerning the values of the thermal expansion coefficient, in the first mode, the gripper will be closed, while in the second mode, the gripper will be opened.

2.2 Optimization using RSM

The RSM is a collection of mathematical and statistical inference approaches used to model and analyse issues where the system's output (solution) is controlled by a large number of variables and the goal is to maximise the given solutions. In the RSM, a series of data obtained via performing experimental and/or numerical tests are used to solve the multivariate equations simultaneously. One of the initial steps in RSM-based optimisation design is settling on an

optimisation model. To do this, the functions that need to be optimised as well as the variables that have the most influence on the functions must be determined.

In the statistical technique of RSM, the model adaptation is carried out through regression analysis. In fact, the RSM is an approximate one which fits the data obtained from the experiments. Assume that the output y (response) is a function of the variables $[x_1, x_2, x_3, \dots, x_k]$. The relationship between the system's outputs and variables can be expressed as [20]:

$$y = f(x_1, x_2, \dots, x_k) + e \quad (1)$$

Here ' e ' stands for the error term in the response determination. Now, if the expected response of the system is expressed as, then the level defined as follows is called the response surface.

$$\eta = f(x_1, x_2, \dots, x_k) \quad (2)$$

The relation between the problem's independent variables and the consequent responses is often not known in RSM issues. Therefore, the first step in finding a RSM is to find an appropriate approximation between the response (y) and the set of independent variables. If the RSM is appropriately modelled with a linear equation of the problem variables, the approximate function will be a first-order model, while for the curvature, polynomials with higher degrees are used. Generally, the polynomial RSM can be given in a matrix form as in Eq. (3).

$$y = xb + e \begin{cases} x = [x_1, x_2, \dots, x_i] \\ b = [\beta_1, \beta_2, \dots, \beta_i] \end{cases} \quad (3)$$

where 'x' is the input matrix and 'b' stands for the vector of coefficients. To estimate the unknown coefficients, a set of variable data and their corresponding set of responses, 'y', are determined. If 'Y' and 'X' represent the set of responses and matrix of variables, respectively, the vector of coefficients is obtained according to Eq. (4).

$$b = (X^T X)^{-1} X^T Y \quad (4)$$

The least-squares method is used in order to estimate the unknown coefficients in the approximate polynomial. To use this method, the number of test specimens must be greater than the unknown coefficients so that the $X^T X$ matrix is not singular [20].

After determining the unknown coefficients, the system response is approximately modelled by the surface fitting to the obtained data. If the surface provides a good approximation of the response function, the analysis of the fitted surface will be equivalent to the real-system analysis considering an acceptable value of error. Given an appropriate design of experiments for the data collection, the coefficients will be determined with higher accuracy and the fitting model's error will be reduced. The designs used for this purpose are called the RSM experiment designs.

According to [14], the control parameters were set at three levels, as shown in Table 2. Therefore, an overall number of

Table 2 Control factors and their levels

Control factors	Levels		
	1	0	- 1
Pre-strain [ε (-)]	0.05	0.2	0.1
Thickness ratio [$t_r = t_i/t_o$ (-)]	2	0.5	1
Temperature [T (°C)]	120	100	80

54 cases were examined. The input parameters include the pre-strain, the thickness ratio of the inner layer to the outer layer, and the temperature applied to the soft gripper. Six various geometries of the bi-stable soft robotic gripper were evaluated since each of the pre-strain and thickness ratio parameters has three levels. Figure 3 shows three grippers with different pre-strain values at a thickness ratio equal to 1. Besides, to examine the amount of effective deformation in the bilayer pre-strain structure and the amount of stability of the structure, two output responses, including the average distance between the two clamps of the gripper and the maximum value of the strain energy, were considered.

2.3 Numerical simulation

In this study, commercial ABAQUS 2017 software was utilized to FEM simulate the soft silicone gripper under different applied thermal loading conditions. For this reason, samples of soft grippers with different thickness ratios and pre-strain values were made with CATIA V5 software (Fig. 3).

A coupled temperature-displacement modelling algorithm was utilized as the simulation problem of the 4D-printed soft gripper is a combination of thermal and mechanical phenomena. Furthermore, to simulate the effects of thermal loading, the time needed for the deformation completion of the soft gripper due to thermal loading was set to be equal to 1 min (60 s). Thermal load was applied to the soft gripper as a constant temperature according to the values specified in Table 2, and the initial temperature of the gripper was set to be equal to 20 degrees Celsius (ambient temperature). Besides, the upper surface of the clamp is fixed at the reference point (RP) in all directions. As shown in Fig. 4, a total of 18,673 triangular 4-node coupled temperature-displacement elements (C3D4T) were used in the present modelling. The size of the elements was chosen so that at least one element is created in the thickness of each structure, and on the other hand, the results are independent of the mesh size.

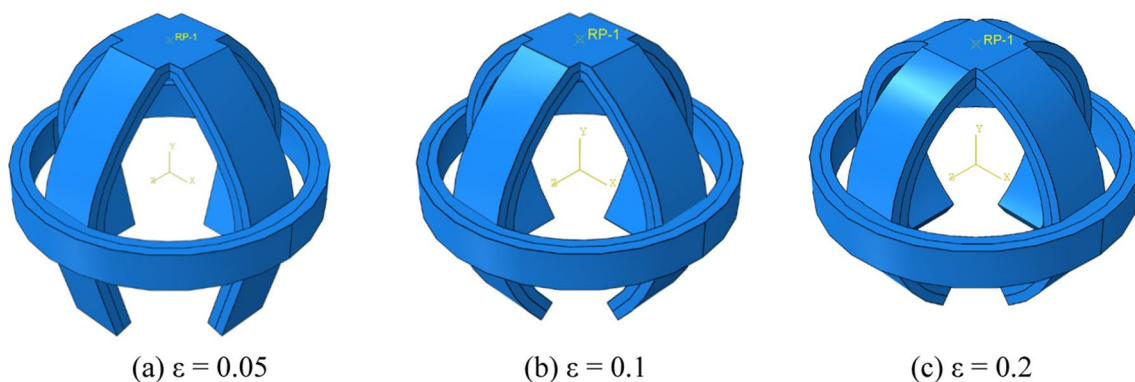


Fig. 3 The bi-stable soft robotic gripper with three various pre-strain values for capturing different sizes of moving targets

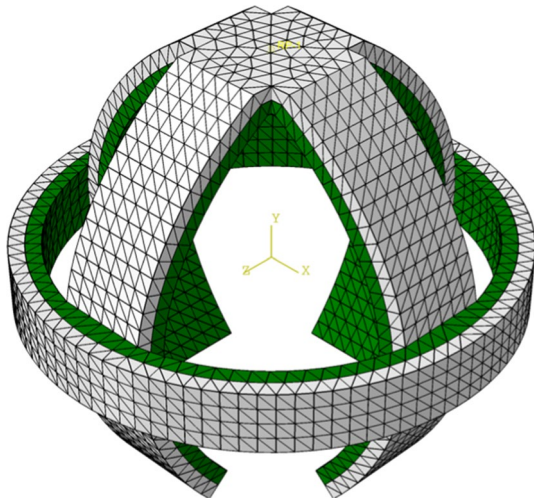


Fig. 4 The meshing scenario for the bi-stable soft robotic gripper analysis

2.4 RSM modelling and optimisation

The RSM methodology is applied for modelling and optimizing the bi-stable soft robotic gripper behaviour under various conditions. So, input parameters, including the values of pre-strain, thickness ratio, and temperature, along with output parameters, such as the maximum strain energy and the average distance between the clamps of the gripper are introduced in Table 2. Two opening and closing modes are also considered in the solution procedure. The output responses of the RSM solution method were extracted following the FEM simulation of the problem. All simulation conditions and their corresponding results are reported in Table 3, where t_r , ϵ , T , α_{in} , α_{out} , E and L are the values of thickness ratio, pre-strain, applied temperature, thermal expansion coefficient of interior material, thermal expansion coefficient of exterior material, maximum strain energy and the average distance between the clamps, respectively.

After extracting the results, it is possible to demonstrate the dependence of the output responses on the input parameters considered by the RSM methodology. Equations 5–8 demonstrate the dependence of the maximum strain energy and the average distance between clamps in two opening and closing modes.

$$E_{\text{closing mode}} = 4.8875 - 0.13324 * \epsilon - 0.91069 * t_r + 2.3398 * T + 0.14749\epsilon^2 + 0.02082 * \epsilon * t_r - 0.044817 * \epsilon * T - 1.076 * t_r^2 - 0.015281 * t_r * T + 0.44775 * T^2 \quad (5)$$

$$L_{\text{closing mode}} = 4.1455 - 1.2966 * \epsilon - 1.3787 * t_r + 1.5141 * T + 0.93574 * \epsilon^2 + 0.54239 * \epsilon * t_r - 0.1379 * \epsilon * T + 0.22892 * t_r^2 + 0.10152 * t_r * T + 0.19013 * T^2 \quad (6)$$

$$E_{\text{opening mode}} = 0.86478 - 1.2645 * \epsilon + 0.24337 * t_r + 0.40821 * T + 0.264828 * \epsilon^2 - 1.0691 * \epsilon * t_r - 0.33487 * \epsilon * T + 0.9117 * t_r^2 + 0.29026 * t_r * T + 0.47515 * T^2 \quad (7)$$

$$L_{\text{opening mode}} = -1.1588 - 3.1232 * \epsilon + 3.3289 * t_r - 0.22836 * T + 3.7614 * \epsilon^2 - 3.1206 * \epsilon * t_r - 0.71623 * \epsilon * T + 1.9993 * t_r^2 - 0.22539 * t_r * T + 0.41524 * T^2 \quad (8)$$

The RSM is able to determine the optimal values of several variables simultaneously with the least amount of data. In this method, the RSM curves are obtained by fitting the appropriate model to the output data. After modelling the responses of the experiments, the most optimal parameters are obtained using the RSM. Equations 5–8 represent the maximum strain energy and the average distance between the clamps for the two opening and closing modes are achieved. Model number 25 corresponds to the most optimal condition for 27 models in opening mode. In this case, the optimal values of maximum strain energy of 1.57341 mJ and the average distance between the clamps of 3.2812 mm have been obtained for Model CCC. Similarly, experiment number 46 corresponds to the most optimal condition for the second 27 experiment models in closing mode. Accordingly, the most optimal values for this condition are the maximum strain energy of 2.19955 mJ and the average distance between the clamps of 2.1654 mm which corresponds to Model C.

3 Results and discussion

3.1 Validation

In order to check the accuracy of the simulation and the effect of the thermal stimulus on the bilayer soft robotic grippers, the present simulation results were compared to those in [14]. A two-layer structure with a bottom layer (ethanol–silicon composite) thickness of 2 mm, top layer (PDMS) thickness of 1 mm, width of 2 cm, a length of 7 cm and a pre-strain of 0.2, at a temperature of 100 °C, having the properties listed in Table 1, is simulated by ABAQUS software. Figure 4 shows the comparison between the von Mises stress contour in the present work and that in [14].

Table 3 Simulation conditions and the obtained results

Case	Problem description						Output parameters	
	t_r	ε	Designation file name	T (°C)	$\alpha_{in} 10^3 (K^{-1})$	$\alpha_{out} 10^3 (K^{-1})$	E (mJ)	L (mm)
1	1	0.1	Model A	80	0	2.5	2.474	3.950
2	1	0.1		100	0	2.5	5.424	5.528
3	1	0.1		120	0	2.5	8.552	7.165
4	0.5	0.1	Model AA	80	0	2.5	5.291	4.348
5	0.5	0.1		100	0	2.5	4.738	7.193
6	0.5	0.1		120	0	2.5	5.044	7.284
7	2	0.1	Model AAA	80	0	2.5	1.502	2.188
8	2	0.1		100	0	2.5	3.008	3.204
9	2	0.1		120	0	2.5	5.290	5.425
10	1	0.2	Model B	80	0	2.5	2.476	2.847
11	1	0.2		100	0	2.5	5.068	3.717
12	1	0.2		120	0	2.5	8.874	4.885
13	0.5	0.2	Model BB	80	0	2.5	2.241	4.159
14	0.5	0.2		100	0	2.5	4.622	4.975
15	0.5	0.2		120	0	2.5	8.019	6.788
16	2	0.2	Model BBB	80	0	2.5	1.464	1.936
17	2	0.2		100	0	2.5	2.939	2.755
18	2	0.2		120	0	2.5	5.174	5.428
19	1	0.05	Model C	80	0	2.5	2.553	5.187
20	1	0.05		100	0	2.5	5.080	7.252
21	1	0.05		120	0	2.5	8.902	9.688
22	0.5	0.05	Model CC	80	0	2.5	2.442	7.572
23	0.5	0.05		100	0	2.5	5.048	8.310
24	0.5	0.05		120	0	2.5	8.830	10.056
25*	2	0.05	Model CCC	80	0	2.5	1.573	3.281
26	2	0.05		100	0	2.5	3.225	4.487
27	2	0.05		120	0	2.5	5.664	6.079
28	1	0.1	Model A	80	2.5	0	1.603	0.924
29	1	0.1		100	2.5	0	1.934	1.122
30	1	0.1		120	2.5	0	1.629	0.937
31	0.5	0.1	Model AA	80	2.5	0	3.394	0.549
32	0.5	0.1		100	2.5	0	3.386	0.616
33	0.5	0.1		120	2.5	0	5.969	1.004
34	2	0.1	Model AAA	80	2.5	0	1.003	5.463
35	2	0.1		100	2.5	0	0.160	1.184
36	2	0.1		120	2.5	0	0.787	1.688
37	1	0.2	Model B	80	2.5	0	0.374	0.053
38	1	0.2		100	2.5	0	0.705	0.194
39	1	0.2		120	2.5	0	0.372	0.066
40	0.5	0.2	Model BB	80	2.5	0	1.350	0.470
41	0.5	0.2		100	2.5	0	1.106	0.069
42	0.5	0.2		120	2.5	0	1.017	0.096
43	2	0.2	Model BBB	80	2.5	0	0.867	4.530
44	2	0.2		100	2.5	0	0.812	4.234
45	2	0.2		120	2.5	0	1.629	0.548
46*	1	0.05	Model C	80	2.5	0	2.199	2.165
47	1	0.05		100	2.5	0	2.312	2.266
48	1	0.05		120	2.5	0	2.269	2.253

Table 3 (continued)

Case	Problem description			Output parameters				
	t_r	ε	Designation file name	T (°C)	$\alpha_{in} 10^3 (K^{-1})$	$\alpha_{out} 10^3 (K^{-1})$	E (mJ)	L (mm)
49	0.5	0.05	Model CC	80	2.5	0	0.993	0.481
50	0.5	0.05		100	2.5	0	0.288	0.146
51	0.5	0.05		120	2.5	0	1.014	0.490
52	2	0.05	Model CCC	80	2.5	0	4.907	15.718
53	2	0.05		100	2.5	0	5.430	15.671
54	2	0.05		120	2.5	0	9.442	21.045

25*the most optimal response for the 27-test simulation in the opening mode

46*the most optimal response for the 27-test simulation in the closing mode

Fig. 5 Comparison of stress contour in the **a** Zou et al. [14] and **b** present work (before and after deformation)

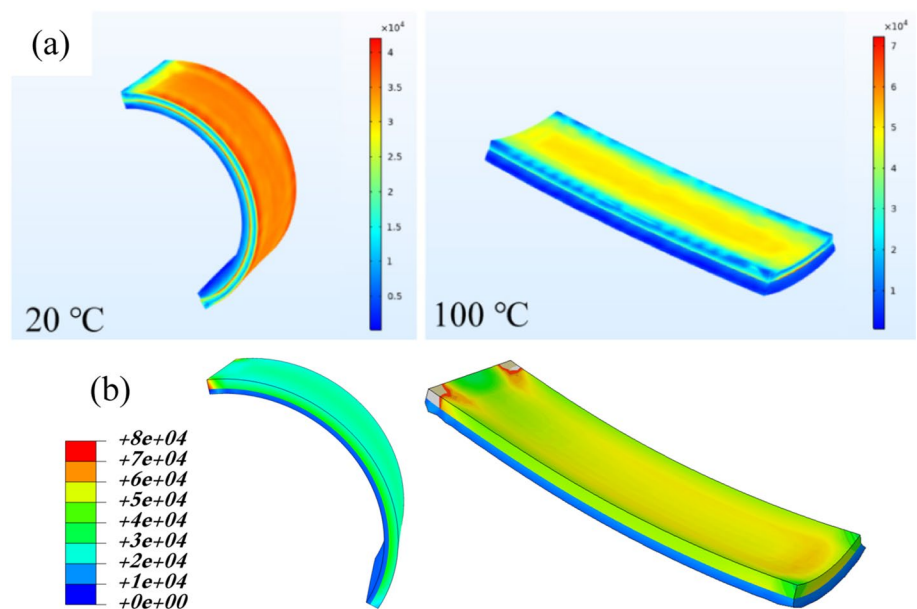


Figure 5 demonstrates the morphing of a bilayer structure with a pre-strain of 0.2, which becomes flat after applying a thermal stimulus, and the highest amount of stress will occur in the middle of the upper surface.

Figure 6 represents the curve variations in terms of temperature changes during the deformation process of the 4D-printed bilayer structure. Figure 5 shows the accuracy and precision of the present simulation results compared to that of the research done by Zhou et al. [14]. Also, according to Fig. 5, the longitudinal curvature (κ_1) of the bilayer structure decreases by increasing the temperature. In fact, the value of the initial pre-strain is reduced due to the method of layering under the thermal stimulus. Consequently, thermal strains cause the initial pre-strain to be neutralized. Hence, the structure becomes completely flat. However, it is noteworthy that if the materials of the layers are moved, the bilayer structure will shrink instead of flattening. Figure 7 shows the variation of the 4D-printed bilayer structure at different time snaps of morphing. It is evident that by increasing the applied thermal load, the longitudinal curvature of

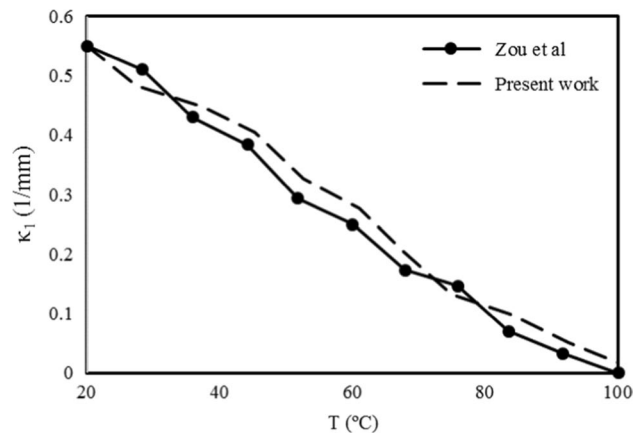


Fig. 6 Variation in the curvature of pre-strained bilayer structure

the bilayer structure gradually decreases. Even though the transverse curvature (κ_2) has gotten bigger over time, the changes in the transverse curvature are not as big as the changes in the longitudinal curvature.

Fig. 7 Deformation of pre-strained bilayer structure (from two views)

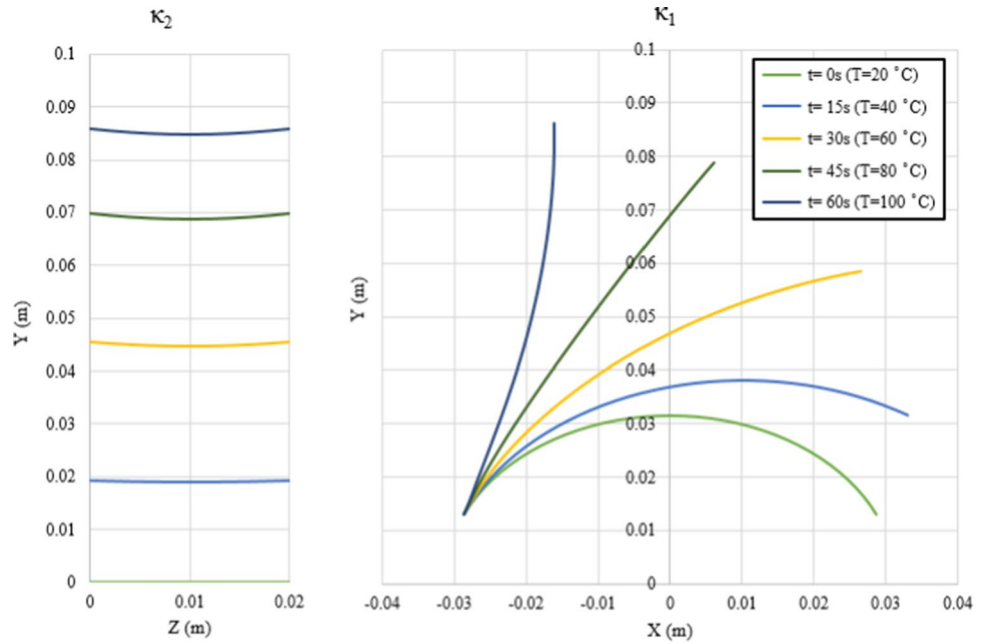


Fig. 8 Comparison of stress contour for pre-strained bi-stable soft robotic gripper (closing mode)

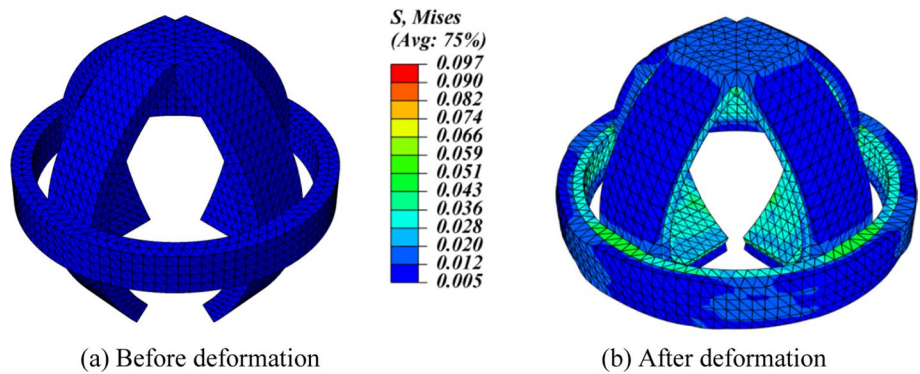
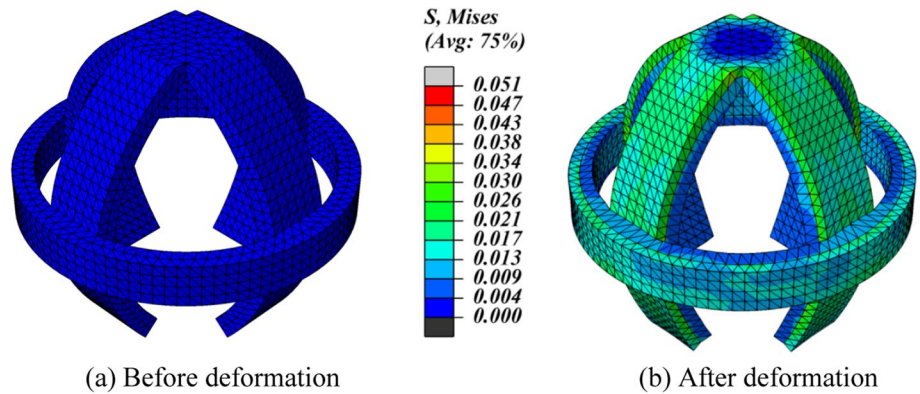


Fig. 9 Comparison of stress contour for pre-strained bi-stable soft robotic gripper (opening mode)



3.2 FEM results

Having validated the simulation results, 54 experiment cases, according to RSM section, are simulated by ABAQUS software, and the output results are listed in Table 3. Figure 8

reports the stress contour of the bi-stable soft gripper with a bilayer structure, with a pre-strain of 0.1, a thickness ratio of 1 and at a temperature of 100 °C in the shrinking state ($\alpha_{in} = 0$), while Fig. 9 shows the stress contour with the same parameters as the opening mode ($\alpha_{out} = 0$).

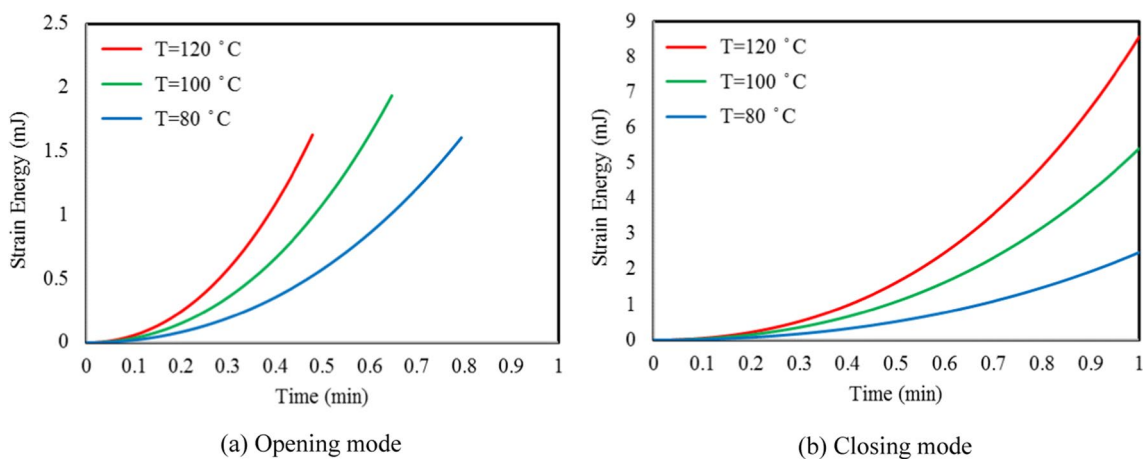


Fig. 10 Strain energy of the pre-strained bi-stable soft robotic gripper

It could be observed that in the shrinking state, or closing mode, ($\alpha_{in}=0$), the stress distribution occurs only in the inner layer of the gripper, and its value is less than 100 kPa, while in the opening mode ($\alpha_{out}=0$), the stress distribution

occurs only in the outer layer of the gripper and its value is less than 50 kPa. It is worth mentioning that in the opening analysis of the bi-stable soft gripper with a bilayer structure, the simulation stops in the middle of the analysis, and the

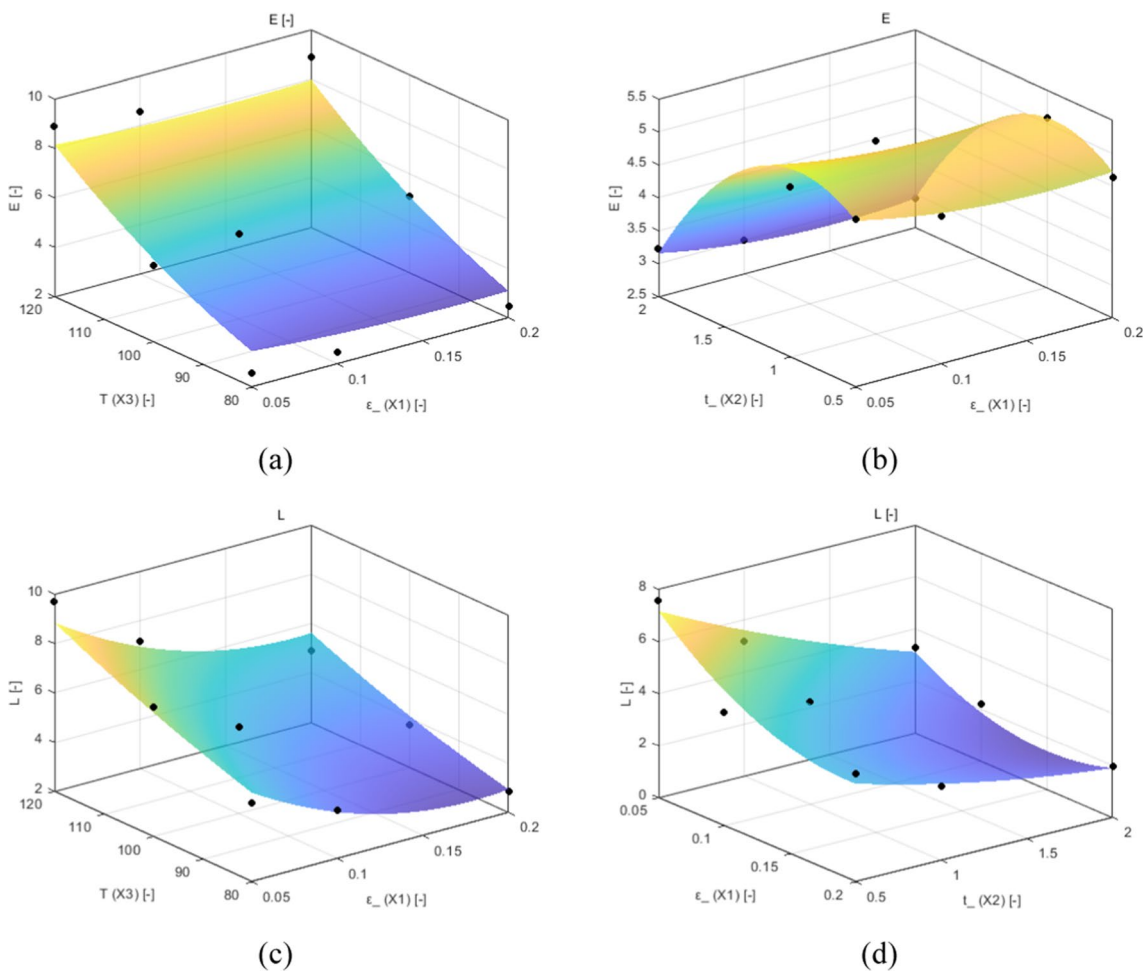


Fig. 11 The interplay of the pre-strain and the a temperature, b thickness ratio values on the maximum strain energy in the opening mode; the pre-strain and the c temperature, d thickness ratio values on the average distance of the gripper clamps in the opening mode

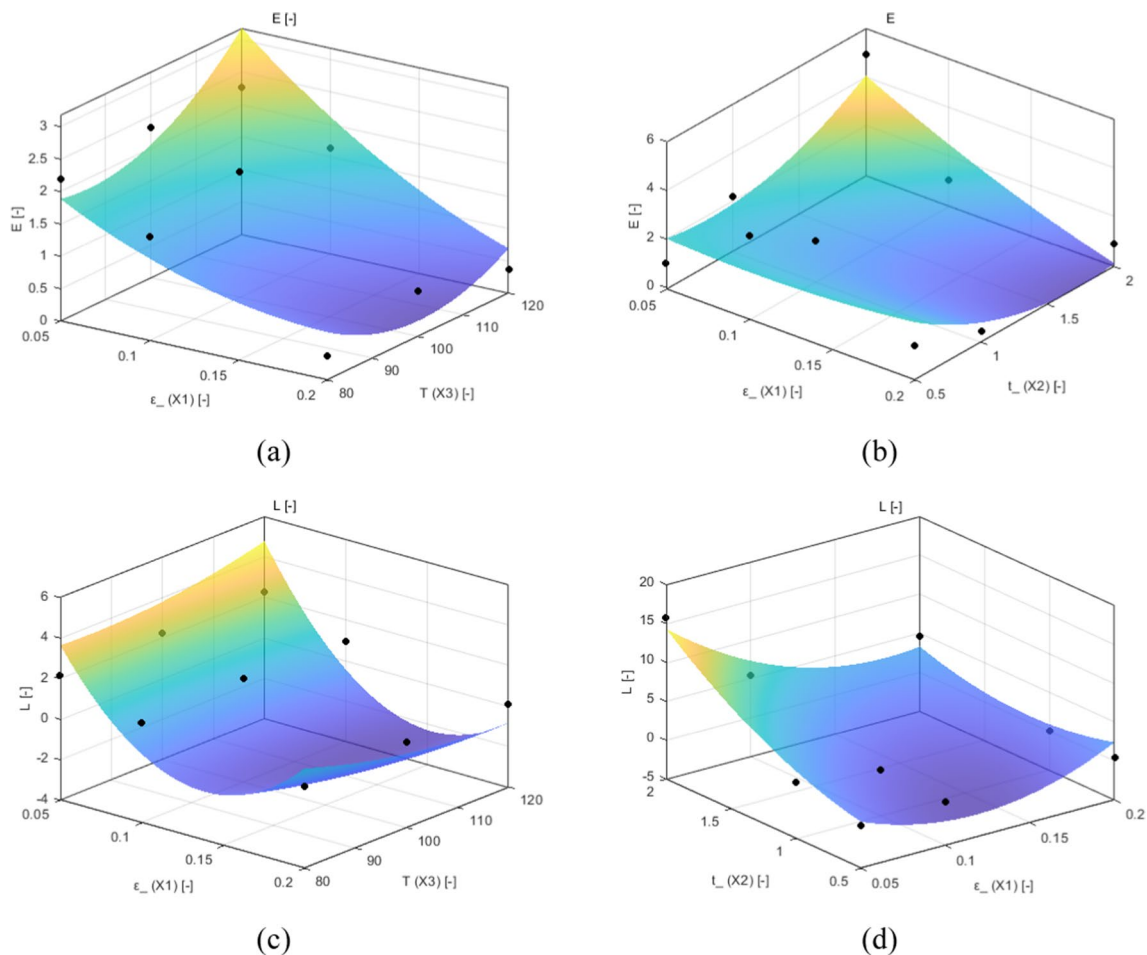


Fig. 12 The interplay of the pre-strain and the **a** temperature, **b** thickness ratio values on the maximum strain energy in the closing mode; the pre-strain and the **c** temperature, **d** thickness ratio values on the average distance of the gripper clamps in the closing mode

time of the process does not exceed 40 s. The reason for this is the presence of a ring around the gripper and the bi-stable mode of the soft gripper. This ring plays the role of controlling the deformation of the gripper and preventing excessive deformations.

Figure 10 shows the strain energy diagram during the deformation process. This figure shows the changes in strain energy during the deformation of the gripper of soft grippers with a pre-strain of 0.1 and a thickness ratio of 1 at different temperatures in both closing and opening modes. Figure 10 also reveals the strain energy changes due to the thermal load applied to the soft grippers in an inadvertent manner. This behaviour of the graph is the same for all 54 models, and only its maximum values are different. Also, it can be seen that increasing the value of temperature applied to the soft gripper increases the strain energy in both the opening and closing modes. As per the results, the gripper in the opening mode does not have the ability to change its shape too much, and the reason is due to the constraint applied from the ring around the bilayer soft gripper. On the

other hand, when the temperature rises, the value of deformation increases, and the ring stops the gripper from further deforming in a shorter time.

3.3 RSM results

The responses of the maximum strain energy and the average distance of the gripper clamps in the RSM with three control levels of pre-strain, thickness ratio and applied temperature for 27 samples in the opening mode and 27 samples in the closing mode are reported in Table 3. This table shows that different gripper models have a significant effect on the control parameters and consequently the responses of the response level method. Using variance analysis, Fig. 11 shows the interaction effects of thickness ratio and applied temperature, respectively, on the maximum strain energy and the average distance of the gripper clamps for the opening modes.

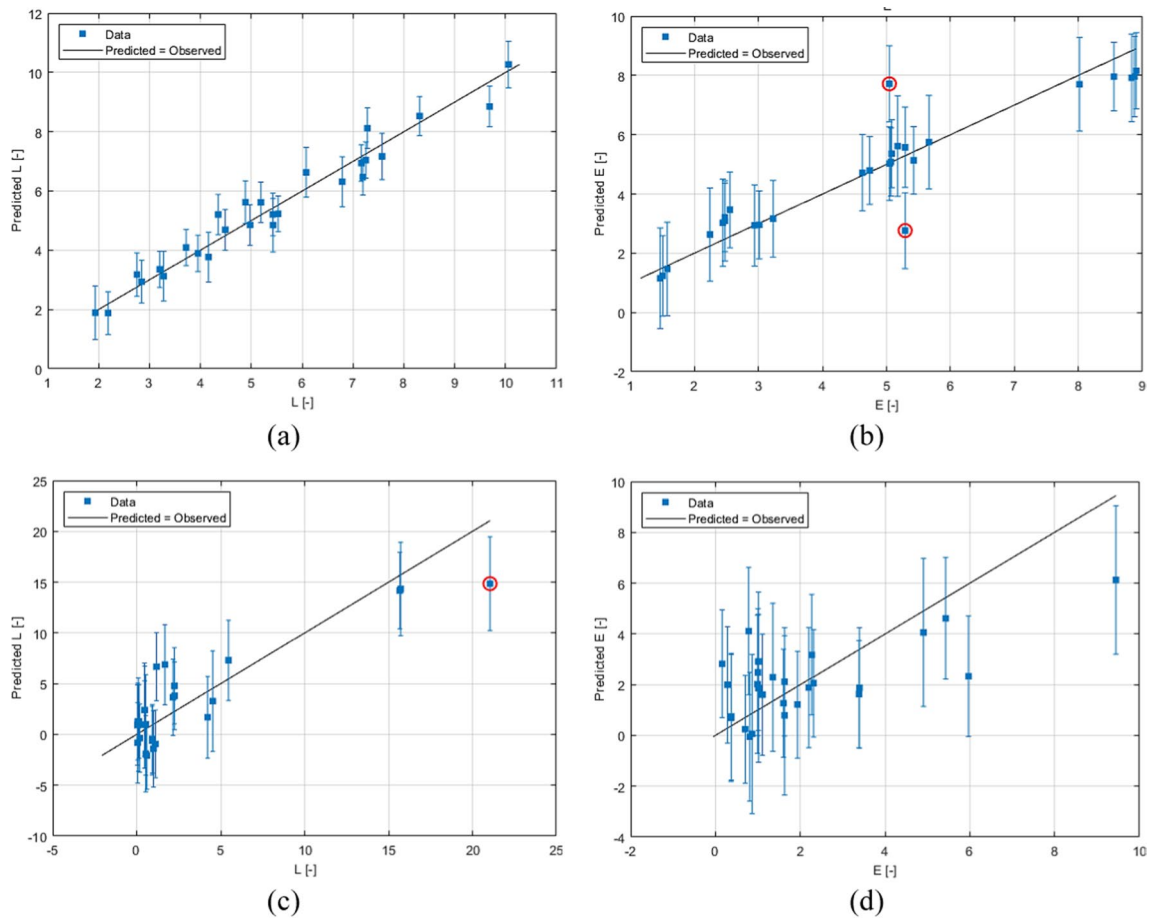


Fig. 13 The predicted diagram of the average distance of the gripper clamps **a** opening mode, **b** closing mode; and the actual and predicted diagram of the maximum strain energy in the **c** opening mode, **d** closing mode

Figure 11 demonstrates that increasing the pre-strain and the thickness ratio or various applied temperatures does not have a significant effect on the maximum strain energy in the opening mode. According to Fig. 10, the average distance of the clamps of the gripper has a parabolic behaviour concerning the pre-strain and the thickness ratio or different applied temperatures: as the thickness ratio decreases, the distance of the clamps increases, and as the temperature increases, the distance between the clamps also increases.

Using variance analysis, Fig. 12 shows the interaction effects of thickness ratio and applied temperature, respectively, on the maximum strain energy and the average distance of the gripper clamps for the closing modes. It is observed that the maximum strain energy in the closing mode is not much affected by increasing the pre-strain and thickness ratio as well as different temperature values. According to Fig. 12, the average distance of the clamps of the gripper has a parabolic behaviour concerning the pre-strain and the thickness ratio or various applied temperatures. In other words, by increasing the temperature or decreasing the thickness ratio, the distance of the clamps

increases. Figure 13 also shows the diagram of predicted values by the RSM for the average distance of the gripper clamps, as well as the maximum strain energy in the closing and opening modes. The red circles indicate some outlier results compared to the predicted values by RSM.

4 Conclusions

The need for a quick and efficient design and optimization approach in the recent development of thermally responsive 4D-printed bi-stable structures in soft robotic applications motivated this study. Hence, a RSM optimization with the aid of numerical solutions to investigate effective parameters in the design of a 4D-printed bi-stable bilayer soft robotic gripper was presented. The (FEM) simulation of the soft silicone gripper under the application of thermal stimulus in different conditions was carried out using ABAQUS software. The soft gripper samples with different material thickness ratios and pre-strain were designed in the CATIA V5 software. Also, experiments were designed based on the

RSM procedure by MATLAB-R2021a software using the MBS Model Fitting Toolbox, which includes three-level variables and two output parameters. After conducting the modelling and optimisation, the most optimal parameters were obtained using the response surface method. The corresponding equations for the maximum strain energy and the average distance of the clamps were obtained for closing and opening modes, concerning pre-strain, thickness ratio and temperature values. According to Table 3 and RSM relationships, the most optimal condition for the opening mode corresponds to model 25 in which the maximum strain energy equals 1.573 mJ and the average distance of the clamps equals 3.281 mm. Likewise, the most optimal condition for the opening mode corresponds to model 46 in which the maximum strain energy of 2.199 and the average distance of the clamps of 2.165 are obtained. This proposed approach was successfully implemented to accelerate the actuation of a thermally responsive model that can be quantitatively controlled by the applied strain and heat stimuli for developing multiscale shape-morphing structures, such as fast buckling and bending, required for soft robotic applications.

Funding Open Access funding enabled and organized by CAUL and its Member Institutions.

Data availability The data that support the findings of this study are available from the corresponding author upon reasonable request.

Open Access This article is licensed under a Creative Commons Attribution 4.0 International License, which permits use, sharing, adaptation, distribution and reproduction in any medium or format, as long as you give appropriate credit to the original author(s) and the source, provide a link to the Creative Commons licence, and indicate if changes were made. The images or other third party material in this article are included in the article's Creative Commons licence, unless indicated otherwise in a credit line to the material. If material is not included in the article's Creative Commons licence and your intended use is not permitted by statutory regulation or exceeds the permitted use, you will need to obtain permission directly from the copyright holder. To view a copy of this licence, visit <http://creativecommons.org/licenses/by/4.0/>.

References

- Zolfagharian A et al (2018) Pattern-driven 4D printing. *Sens Actuators A* 274:231–243
- Bodaghi M et al (2019) 4D printing self-morphing structures. *Materials* 12(8):1353
- Yarali E et al (2022) Magneto-/electro-responsive polymers toward manufacturing, characterization, and biomedical/soft robotic applications. *Appl Mater Today* 26:101306
- Zolfagharian A et al (2022) 3D-printed programmable mechanical metamaterials for vibration isolation and buckling control. *Sustainability* 14(11):6831
- Mohammadi M et al (2022) 4D printing of soft orthoses for tremor suppression. *Bio-Des Manuf* 5:1–22
- Hamzehei R et al (2022) 4D metamaterials with zero poisson's ratio, shape recovery, and energy absorption features. *Adv Eng Mater* 24(9):2200656
- Gul JZ et al (2017) Omni directional multimaterial soft cylindrical actuator and its application as a steerable catheter. *Soft Rob* 4(3):224–240
- Bikas H, Stavropoulos P, Chryssolouris G (2016) Additive manufacturing methods and modelling approaches: a critical review. *Int J Adv Manuf Technol* 83:389–405
- Zolfagharian A, Kaynak A, Kouzani A (2020) Closed-loop 4D-printed soft robots. *Mater Des* 188:108411
- Atalay O et al (2018) A highly sensitive capacitive-based soft pressure sensor based on a conductive fabric and a microporous dielectric layer. *Adv Mater Technol* 3(1):1700237
- Banerjee H, Pusalkar N, Ren H (2018) Single-motor controlled tendon-driven peristaltic soft origami robot. *J Mech Robot*. <https://doi.org/10.1115/1.4041200>
- Tawk C, Mutlu R, Alici G (2021) A 3D printed modular soft gripper integrated with metamaterials for conformal grasping. *Front Robot AI*. <https://doi.org/10.3389/frobt.2021.799230>
- Le Chau N et al (2022) Structural optimization of a rotary joint by hybrid method of FEM, neural-fuzzy and water cycle-moth flame algorithm for robotics and automation manufacturing. *Robot Auton Syst* 156:104199
- Zou Y et al (2021) 4D printing pre-strained structures for fast thermal actuation. *Front Mater* 8:661999
- Deng H et al (2020) 4D printing elastic composites for strain-tailored multistable shape morphing. *ACS Appl Mater Interfaces* 13(11):12719–12725
- Liu Y et al (2023) A soft and bistable gripper with adjustable energy barrier for fast capture in space. *Soft Robot* 10:77
- Zolfagharian A et al (2022) Silicon-based soft parallel robots 4D printing and multiphysics analysis. *Smart Mater Struct* 31(11):115030
- Thuruthel TG et al (2020) A bistable soft gripper with mechanically embedded sensing and actuation for fast grasping. In: 2020 29th IEEE International Conference on Robot and Human Interactive Communication (RO-MAN)
- Schneider F et al (2009) Process and material properties of polydimethylsiloxane (PDMS) for Optical MEMS. *Sens Actuators A* 151(2):95–99
- Kini SD (2004) An approach to integrating numerical and response surface models for robust design of production systems. The Ohio State University

Publisher's Note Springer Nature remains neutral with regard to jurisdictional claims in published maps and institutional affiliations.